Chapter 6
Light Scattering by Small Particles and Their Light Heating: New Aspects of the Old Problems

Michael I. Tribelsky and Boris S. Luk'yanchuk

Abstract A survey of recent results in light scattering by nanoparticles is presented. Special attention is paid to the case of particles from weakly dissipating materials, when the radiative damping prevails over the dissipative losses. It makes the scattering process completely different from the Rayleigh one. Peculiarities of the energy circulation in the near field zone are inspected in detail. The problem of optimization of the energy release in the particle is discussed. The chapter is concluded with consideration of laser heating of a metal particle in liquid important for biological and medical applications.

6.1 Introduction

Since the first quantitative study by Lord Rayleigh [1], the problem of light scattering by small particles has remained one of the most important and appealing issues of electrodynamics. There are thousands of articles and numerous monographs devoted to this subject, see, e.g., [2–5] and references therein. Plasmon (polariton) resonances and their role in the light scattering, as well as a related issue of interplay between radiative and dissipative damping are not new too [6], but they still remain topics of intense study [7–9].

M. I. Tribelsky
Faculty of Physics, Lomonosov Moscow State University, Moscow 119991, Russia

M. I. Tribelsky (✉)
Moscow State Institute of Radioengineering, Electronics and Automation (Technical University MIREA), Moscow 119454, Russia
e-mail: tribelsky@mirea.ru

B. S. Luk'yanchuk
Data Storage Institute, Agency for Science, Technology and Research, Singapore 117608, Singapore
e-mail: Boris_L@dsi.a-star.edu.sg

V. P. Veiko and V. I. Konov (eds.), *Fundamentals of Laser-Assisted Micro- and Nanotechnologies*, Springer Series in Materials Science 195,
DOI: 10.1007/978-3-319-05987-7_6,

Regarding absorption of light by small plasmonic nanoparticles, it is a key effect for numerous applications of nanostructures in data storage technology, nanotechnology, chemistry, medicine, biophysics and bioengineering. The absorption characteristics depend on the material of the particle and its shape. It is sufficed mentioning absorption enhancement in amorphous silicon nanocone arrays [10]. Properties of such black silicon are useful for a wide range of commercial devices. Recently the problem of laser heating of plasmonic nanoparticles has attracted a lot of attention too (see, e.g., [11–20] and references therein). A similar problem arises in astrophysics with thermal noise in interstellar dust, where temperature fluctuations for small particles of interstellar dust may be about 1000 K [21]).

Various aspects of laser and laser-enhanced production of such particles, their properties and applications are discussed in Chaps. 4, 5 and 8 of the present monograph. In this chapter a survey of recent results in light scattering by small (relative to the wavelength of the incident light λ) spatially uniform nonmagnetic spherical nanoparticles and their laser heating is presented. We reveal a number of paradoxical, counterintuitive features of the problem, which shed new light on these important phenomena.

First, the problem of the so-called *anomalous light scattering* is discussed. The anomalous scattering may be realized close to the plasmon resonance frequencies, provided the dissipative losses are small enough. It is shown that despite the smallness of the particle the phenomenon has very little in common with the Rayleigh scattering. The most attention is paid to the discussion of the Poynting vector near-field structure, which occurs rather complicated. It includes a number of singular points, while the energy flow is divided into various branches of different shapes and orientations. In this case fine variations of the incident light frequency may result in global changes of the near-field structure.

Then, the problem of optimization of light absorption by a nanopartile is discussed in detail. It is shown that counter-intuitively the maximal absorption is achieved for a particle with a *small* value of the dissipative constant. A simple universal formula describing the absorption line shape as a function of complex dielectric permittivity of the particle is presented. Close to plasmon resonances the particle acts as a funnel, collecting the incident light from rather a broad area and delivering it to the near field zone. As a result the local field inside the particle (and hence the dissipation rate) may increase dramatically relative to the ones for the same material in bulk. We introduce a new quantity, the *effective volume absorption coefficient* α_{eff} of the particle, which allows to compare the dissipation rates in the particle and the corresponding bulk material quantitatively. Such a comparison is performed for a number of metals. It allows to find the optimal size of the particle and its optimal material to achieve the maximal energy release.

Next, we consider the general problem of laser pulse heating of a spherical metal particle embedded in a host medium, taking into account heat transfer from the particle to the environment. We employ the exact Mie solution of the diffraction problem and solve heat-transfer equations to determine the maximum temperature rise at the particle surface as a function of the optical and thermometric parameters of the problem. The main attention is paid to the case when the thermal diffusivity of the particle

is much larger than that of the environment (metal particles in liquids, e.g., in water and alike). We show that in this case at any given duration of the laser pulse the maximal temperature rise as a function of the particle size reaches an absolute maximum at a certain finite size of the particle. Simple approximate analytical expressions for this dependence, which cover the entire range of the problem parameters and agree well with the direct numerical simulation are presented.

In conclusion we summarize the main points of the issues discussed.

6.2 Anomalous Light Scattering

6.2.1 General Principles

The conventional reasoning employed to describe light scattering by a small uniform nonmagnetic spherical particle, which may be found in any textbook, is as follows. If the particle is small relative to the wavelength of the incident light, the electric field of the latter, which "feels" the particle, is practically spatially homogeneous. The homogeneous field produces just a dipole polarization, oscillating in time with the frequency of the incident light ω. Any oscillating dipole emits electromagnetic waves. In our case these waves are precisely what the scattered light is. Then, recollecting the well known expression for the polarizability of a sphere with a given permittivity by a uniform electric field [22], we immediately arrive at the famous Rayleigh formula for the scattering cross section σ_{sca}:

$$\sigma_{\mathrm{sca}} = \frac{8}{3}\pi R^2 q^4 \left|\frac{\varepsilon - 1}{\varepsilon + 2}\right|^2; \quad q = \frac{2\pi R}{\lambda} \ll 1, \tag{6.1}$$

where R is the particle radius and $\varepsilon = \varepsilon_p/\varepsilon_m$ stands for the relative permittivity of the particle. Here ε_p and ε_m mean the absolute permittivities of the particle and host medium, respectively. Note, that while the permittivity of the particle, generally speaking, is complex, the one for the host medium is supposed to be a purely real positive quantity.

Divergence of the denominator in (6.1) at $\varepsilon = -2$ is a well known fact. It corresponds to a resonant excitation of localized plasmons, whose eigenfrequency ω_1 (the meaning of subscript 1 will be clear later on) is defined through the dispersion law $\mathrm{Re}\,\varepsilon(\omega_1) = -2$, while $\mathrm{Im}\,\varepsilon \neq 0$ provides a finite cutoff for the divergence.

Note now, that though the mentioned cutoff always prevents the divergence of σ_{sca}, it is not always meaningful. If $\mathrm{Im}\,\varepsilon$ is very small $\sigma_{\mathrm{sca}}(\omega_1)$ may become extremely large, so that a nanoparticle may have the scattering cross section equal to, say, several square kilometers, which, of course, cannot be the case. The point is that apart dissipative losses the problem in question has an additional cutoff mechanism, namely the inverse transformation of localized plasmons into traveling electromagnetic waves or, in other words, the radiative damping. Its grounds are related to the fact that

the scattered light is the radiation emitted owing to oscillations of the eigenmodes excited in the particle by the incident light. Since the emitted waves take off energy, the eigenmodes are damped even if the dissipative losses do not exist at all. This non-dissipative damping is a very weak effect, which usually may be neglected. The neglect corresponds to the Rayleigh approximation and yields (6.1). However, if the dissipation is weak itself, the radiative damping may become the major mechanism of the cutoff.

It should be stressed that the radiative damping and its role in the cutoff is well known for a very long time. We could find a reference to it in paper [23] published in 1951 (!), though we are not sure that this is the very first mentioning of the effect. However, what has been overlooked is the fact that when the radiative damping begins to prevail over the dissipative one, the entire scattering process undergoes drastic changes. For this reason we have singled out this type of light scattering into a separate class, naming it the *anomalous scattering*. The goal of the present section is to elucidate various features of the anomalous scattering and their consequences.

To this end, we have to go beyond the Rayleigh approximation. Fortunately, there is the exact solution to the problem of light diffraction by a sphere, known as the Mie solution, see e.g. [2, 3]. According to the solution the scattered electromagnetic wave is presented as a superposition of waves emitted by an infinite number of multipoles excited in the sphere by the incident wave. The net extinction, scattering and absorption efficiencies (the corresponding cross sections normalized over the geometrical cross section of the sphere) in this case equal to

$$Q_{\text{ext, sca, abs}} = \sum_{l=1}^{\infty} Q^{(\ell)}_{\text{ext, sca, abs}}, \tag{6.2}$$

where the *partial efficiencies* $Q^{(\ell)}_{\text{ext, sca, abs}}$ are expressed in terms of the scattering coefficients a_ℓ, b_ℓ:

$$Q^{(\ell)}_{\text{ext}} = \frac{2(2\ell+1)}{q^2}\text{Re}(a_\ell + b_\ell), \;\; Q^{(\ell)}_{\text{sca}} = \frac{2(2\ell+1)}{q^2}(|a_\ell|^2 + |b_\ell|^2). \tag{6.3}$$

Each partial efficiency corresponds to the radiation of the ℓth order multipole, and terms proportional to a_ℓ and b_ℓ in (6.3) describe the radiation related the to electric and magnetic polarizabilities, respectively.

Regarding the absorption efficiency, in accord with the energy conservation law $Q_{\text{abs}} = Q_{\text{ext}} - Q_{\text{sca}}$. Since radiation of each multipole is independent, the same relation is valid for the partial efficiencies too, i.e.,

$$Q^{(\ell)}_{\text{abs}} = Q^{(\ell)}_{\text{ext}} - Q^{(\ell)}_{\text{sca}} \tag{6.4}$$

Thus, for the problem in question the key quantities are a_ℓ, b_ℓ. They may be presented in the form:

$$a_\ell = \frac{F_\ell^{(a)}(q,\varepsilon)}{F_\ell^{(a)}(q,\varepsilon) + iG_\ell^{(a)}(q,\varepsilon)},\quad b_\ell = \frac{F_\ell^{(b)}(q,\varepsilon)}{F_\ell^{(b)}(q,\varepsilon) + iG_\ell^{(b)}(q,\varepsilon)}, \tag{6.5}$$

where $F_\ell^{(a,b)}$, $G_\ell^{(a,b)}$ are expressed in terms of the Bessel $[J_{l+1/2}(\zeta)]$ and Neumann $[N_{l+1/2}(\zeta)]$ functions. The corresponding general expressions are rather cumbersome and are not be presented here. They may be found, e.g., in [2, 3].

In what follows we will focus on light scattering by a small particle, when $q \ll 1$, see (6.1). In this case the general expressions for $F_\ell^{(a,b)}$, $G_\ell^{(a,b)}$ may be expended in powers of small q. The expansion yields

$$F_\ell^{(a)}(q,\varepsilon) \simeq q^{2\ell+1}\frac{\ell+1}{[(2\ell+1)!!]^2}(\varepsilon-1)+\cdots \tag{6.6}$$

$$G_\ell^{(a)}(q,\varepsilon) \simeq \frac{\ell}{2\ell+1}\left\{\varepsilon+\frac{\ell+1}{\ell}-q^2\frac{\varepsilon-1}{2}\left[\frac{\varepsilon}{2\ell+3}+\frac{\ell+1}{\ell\,(2\ell-1)}\right]+\ldots\right\}, \tag{6.7}$$

where ellipses denote omitted higher order in q terms. We do not need the corresponding expressions for $F_\ell^{(b)}$, $G_\ell^{(b)}$ because estimates show that for the case in question $|b_\ell|$ is always small relative to $|a_\ell|$, so that the radiation of magnetic multipoles may be neglected [2, 3].

Note, that $|F_\ell^{(a)}| \ll 1$, while $|G_\ell^{(a)}|$, generally speaking, is of the order of unity. Then it seems, that $F_\ell^{(a)}$ in the denominator of (6.5) may be neglected relative to $iG_\ell^{(a)}$. The neglect yields the estimates $Q_{\text{ext}}^{(1)} \gg Q_{\text{ext}}^{(2)} \gg Q_{\text{ext}}^{(3)} \gg \cdots$ and the same for $Q_{\text{sca,abs}}^{(\ell)}$, see (6.3)–(6.5). Thus, we have obtained that the scattering efficiencies are overwhelmingly determined by the electric dipole mode with $\ell = 1$, which in the leading approximation eventually brings about (6.1).

However, this reasoning becomes invalid at the vicinity of the points $\varepsilon = \varepsilon_\ell$, where ε_ℓ are roots of the equations $G_\ell^{(a)}(\varepsilon) = 0$. At any ℓ there is at least one root of this equations,[1] namely

$$\varepsilon_\ell = -\frac{\ell+1}{\ell} + O(q^2), \tag{6.8}$$

see (6.7). As well as it has been discussed above for the dipole resonance at $\ell = 1$, the quantities ε_ℓ at any ℓ through the dispersion law $\varepsilon(\omega)$ define frequencies of the ℓth order plasmon resonance ω_ℓ. The neglect of $F_\ell^{(a)}$ in the denominator of (6.5) in the vicinity of the plasmon resonance results in divergence of a_ℓ at $\varepsilon = \varepsilon_\ell$, cf. (6.1). In contrast to that the exact expression (6.6) yields $a_\ell(\varepsilon_\ell) = 1$, which gives rise to

[1] Actually, at any ℓ the equation $G_\ell^{(a)}(\varepsilon) = 0$ has an infinite number of roots. The roots different from (6.8) correspond to large values of ε and lie beyond the validity range of (6.7). Interference of modes with the same ℓ related to different such roots may result in new interesting phenomena, including cloaking of the particle (the complete suppression of the scattering, which makes the particle invisible), see [24]. However, discussion of these matters lies beyond the scope of the present chapter.

the following finite value for the partial cross sections $\sigma^{(\ell)} = \pi R^2 Q^{(\ell)}$:

$$\sigma_{\rm ext}^{(\ell)} = \sigma_{\rm sca}^{(\ell)} = (2\ell+1)\frac{2\pi}{k^2}, \tag{6.9}$$

see (6.3). As it has been already mentioned above, the physical meaning of the cutoff of the divergency is related to the inverse transformation of resonant localized plasmons, excited in the particle by the incident electromagnetic wave, into scattered light.

Regarding the values of all other off resonant partial extinction (scattering) cross sections, these quantities are defined by the usual Rayleigh approximation, which corresponds to the mentioned neglect of $F^{(a)}$ in the denominator of (6.5). Then, it is seen straightforwardly that at $\varepsilon = \varepsilon_\ell$ the contribution of expression (6.9) to the net cross section is overwhelming.

Equation (6.9) exhibits what we call *the inverted hierarchy of resonances* [25, 26]. In the conventional cases the partial cross sections of high order resonances for a small particle are dying off sharply with an increase in ℓ as has been mentioned above: $\sigma_{\rm ext}^{(\ell)} \sim q^{2(2\ell+1)}$, see (6.3)–(6.7). In contrast, (6.9) yields an increase of the resonant cross section with an increase in ℓ, so that the resonant dipole cross section occurs smaller than the one for the quadrupole resonance, the latter is smaller than the resonant octupole cross section, etc.[2]

In the vicinity of the resonance we may write $F_\ell^{(a)}(\varepsilon) \simeq F_\ell^{(a)}(\varepsilon_\ell)$, $G_\ell^{(a)}(\varepsilon) \simeq (dG_\ell^{(a)}/d\varepsilon)_{\varepsilon_\ell}(d\varepsilon/d\omega)_{\omega_\ell}\delta\omega$, where $\delta\omega = \omega - \omega_\ell$. It immediately brings about the conventional Lorenzian profile for $\sigma_{\rm ext}(\omega)$ with the full-width at half-maximum (FWHM) [26]

$$\gamma_\ell = \frac{2q^{2\ell+1}(\ell+1)}{[\ell(2\ell-1)!!]^2(d\varepsilon/d\omega)_{\omega_\ell}}, \tag{6.10}$$

see (6.3). Note a sharp decrease in the linewidth with an increase in ℓ.

The next point to be made is independence of the resonant cross section (6.9) of the particle size R. It gives rise to the paradoxical conclusion that a particle with $R = 0$ still has a finite extinction cross section. We face the paradox because in our consideration we have neglected dissipative processes entirely. Meanwhile dissipation never can vanish completely, and hence the linewidth (6.10) related to the radiative damping cannot be smaller than the natural linewidth determined by the dissipation. When the latter becomes comparable with the former, (6.9) becomes invalid and the conventional Rayleigh scattering is restored. It results in the following applicability conditions for the anomalous scattering to come into being [27][3]:

---

[2] The inverted hierarchy does not affect convergence of the multipole expansion because each resonance takes place at its own resonant value of ε, so that at a given order of the resonance we have just a single partial cross section describing by (6.9).

[3] Usually, taking into account sign of strong inequality in (6.11), $(\ell+1)/\ell$ in its right-hand-side is replaced by 1. Here we do not do that because it is important for the anomalous absorption, which will be discussed in the next section.

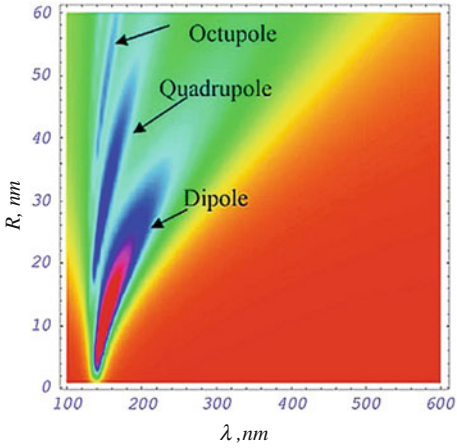

Fig. 6.1 The extinction cross section of a spherical aluminum particle in a vacuum. The exact Mie solution and actual optical properties of aluminum

$$\varepsilon''(\omega_\ell) \ll q^{2\ell+1} \frac{\ell+1}{[\ell(2\ell-1)!!]^2}, \tag{6.11}$$

where ε'' stands for Im ε.

Thus, to observe the anomalous scattering Im ε at the resonant frequency should be small. However, no matter how small Im ε is, at small enough q the condition (6.11) is violated, the Rayleigh scattering is restored, and the extinction cross section tends to zero at $q \to 0$, as it should be.

It is worthwhile stressing that, actually, the condition (6.11) is too strict. Thus, while for a particle with $q = 0.3$ at $\ell = 1$ (6.11) reads $\varepsilon'' \ll 0.03$, in fact the complete restoration of the Rayleigh scattering occurs only at $\varepsilon'' > 0.6$ [28].

As an example, the extinction cross section of a spherical aluminum particle in a vacuum calculated based upon the exact Mie solution is presented in Fig. 6.1. Aluminum is selected owing to small ($\sim$0.1) values of ε'' in the range of the frequencies of its plasmon resonances. To obtain these results the following model has been employed [25]. The empirical dependence ε on ω (known as a table [29]) is approximated by the Drude formula:

$$\varepsilon = 1 - \frac{\omega_p^2}{\omega^2+\gamma^2} + i\frac{\gamma\omega_p^2}{\omega(\omega^2+\gamma^2)}. \tag{6.12}$$

To enhance the accuracy, quantities ω_p and γ, regarded as functions of ω, are calculated at every point in the table with a polynomial interpolation between the points. To take into account collisions of free electrons with the particle surface, $\gamma(\omega)$ found for bulk aluminum is replaced by $\gamma_{\text{eff}} = \gamma(\omega) + v_F/R$, where $v_F = 10^8$ cm/s stands for the Fermi velocity of the free electrons.

In accord with what has been said above, while at $R > 30$ nm the extinction cross section at the quadrupole resonance is larger than that at the dipole one (the inverted hierarchy at the anomalous scattering) the conventional hierarchy of the resonances is restored with a decrease in R. Finally, at $R \to 0$ the cross section vanishes in agreement with the dependence describing the Rayleigh scattering.

6.2.2 Near Field Effects

However, the most appealing manifestation of the anomalous scattering takes place in the near field zone. The key point is that the dramatic changes in both the modulus and phase of the complex amplitude a_ℓ in the vicinity of the plasmon resonances at the anomalous scattering relative to that at the conventional Rayleigh approximation brings about the corresponding dramatic changes in the near-field structure.

We recall that at the anomalous scattering the dissipative losses are negligible, the extinction cross section approximately equals the scattering one and both do not depend on R, see (6.9). On the other hand, by definition the scattering cross section is the overall scattered power [W] normalized over the intensity of the incident wave [W/cm^2]. If for a given incident wave we decrease the geometrical size of a scatterer, and the decrease does not affect the overall scattered power, it means that the characteristic value of the electromagnetic field in the particle should increase to provide the same emitted power from a smaller volume. In other words, at the anomalous scattering the electromagnetic field in the particle and its immediate vicinity should be *singular in q*. This is the case indeed. Utilizing the exact Mie solution and bearing in mind that at the point of the resonances the corresponding $a_\ell = 1$, we can readily obtain the following estimates for the components of the electric $\boldsymbol{E}(\boldsymbol{r})$, magnetic $\boldsymbol{H}(\boldsymbol{r})$ fields and the time-averaged Poynting vector $\langle \boldsymbol{S}(\boldsymbol{r}) \rangle$ in the particle and its near field zone [30]:

$$\frac{E_{r,\varphi,\theta}}{E_0} \sim q^{-(\ell+2)};\ \frac{H_r}{E_0} \sim q^{\ell+1};\ \frac{H_{\varphi,\theta}}{E_0} \sim q^{-(\ell+1)};\ \frac{\langle S_{r,\varphi,\theta} \rangle}{\langle S_0 \rangle} \sim q^{-(2\ell+3)}, \quad (6.13)$$

where subscripts $r,\ \varphi,\ \theta$ designate the corresponding components and E_0, $\langle S_0 \rangle$ stand for the values of E, $\langle S \rangle$ in the incident wave. The time-averaged Poynting vector $\langle \boldsymbol{S}(\boldsymbol{r}) \rangle$, as usual, is defined as follows [2, 3]:

$$\langle \boldsymbol{S} \rangle = \frac{c}{8\pi} \langle \mathrm{Re}[\boldsymbol{E} \times \boldsymbol{H}^*] \rangle. \quad (6.14)$$

We remind for reference that at the conventional scattering (the Rayleigh approximation) $a_\ell \sim q^{2\ell+1}$ [2, 3]. For the near field zone instead of (6.13) it yields

$$\frac{E_{r,\varphi,\theta}}{E_0} \sim q^{\ell-1};\ \frac{H_r}{E_0} \sim q^{\ell+1};\ \frac{H_{\varphi,\theta}}{E_0} \sim q^{\ell};\ \frac{\langle S_{r,\varphi,\theta} \rangle}{\langle S_0 \rangle} \sim q^{2\ell}. \quad (6.15)$$

Let us stress the dramatic difference between (6.13) and (6.15). If for the latter the electromagnetic field in the particle and its vicinity vanishes sharply when $q \to 0$, for the former it (but component H_r) *increases sharply* with a decrease in q, as long as the approximation of the anomalous scattering holds.[4] Physical grounds for this unusual behavior will be clear if we elucidate the detailed structure of the electromagnetic field in the near field zone. To this end, we need a certain geometrical description of the field structure.

The characteristic spatial scale of the problem is much smaller than the wavelength of the incident light. Therefore, we cannot use the convenient and visual way to show the propagation of light by optical rays, applicable only in the opposite limit of the geometrical optics. However, instead of that we can show the energy circulation in the near field, plotting field lines of the time-averaged Poynting vector. The spatial dependence of electric $\boldsymbol{E}(\boldsymbol{r})$ and magnetic $\boldsymbol{H}(\boldsymbol{r})$ fields, entering in (6.14), are given by the exact Mie solution. Thus, drawing the field lines of $\langle \boldsymbol{S}(\boldsymbol{r}) \rangle$ is a straightforward but quite laborious matter. Details of the corresponding algorithms may be found, e.g., in [2, 28].

Study of the structure of the vector Poynting field in the near field zone [25, 26, 28, 31–33] shows that in the vicinities of the plasmon resonances it is very complicated and includes singular points, whose number and positions are very sensitive to the detuning of the ω from ω_ℓ. The structure depends significantly on the order of the resonance and the dissipation rate in the particle. Though the general picture of the dependence of the structure on the entire set of the problem parameters is not clear yet, the results obtained allow to conclude that the rate of complexity of the structure decreases with an increase in $\varepsilon''(\omega_\ell)$. Thus, the extreme case is the near field structure in the non-dissipative limit.

As an example, the field lines of $\langle \boldsymbol{S}(\boldsymbol{r}) \rangle$ at the vicinity of the dipole resonance at $q = 0.3$ in the non-dissipative limit are presented in Fig. 6.2 [33]. Generally speaking, the field lines are essentially 3D curves. However, owing to the problem symmetry, the plane $y = 0$ is invariant, i.e., if any non-singular point of a field line belongs to this plane, the entire line belongs to the plane too. It reduces the field structure in this plane to a 2D picture.

It is seen from Fig. 6.2 that the particle acts as a funnel, collecting the energy flux from a large "upstream" area bounded by the red separatrixes of saddle points 1,2 and delivering the energy to the immediate vicinity of the particle. The smaller the particle, the greater the ratio of the diameter of the "inlet" of the funnel to the one of the "outlet" and hence the greater the field concentration at the "outlet." This is the physical reason explaining the mentioned singular in q dependence of

[4] The conventional dependence $H_r(q)$ at the anomalous scattering is explained by the fact that this type of the scattering corresponds to a resonant excitation of eigenmodes related to electric polarizability of the particle. For these modes $H_r = 0$ [2, 3]. Non-zero values of H_r in the near field correspond to the contribution of the magnetic modes, related to the magnetic polarizability of the particle by the electromagnetic field of the incident wave. For a non-magnetic particle these modes always are non-resonant and therefore have the same amplitude both at the anomalous and Rayleigh scattering.

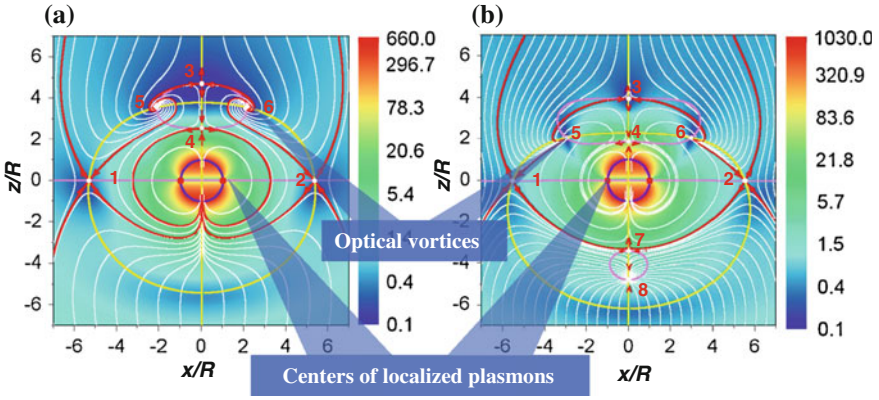

Fig. 6.2 Color density plot of modulus of the time-averaged Poynting vector $\langle \boldsymbol{S}(\boldsymbol{r})\rangle$ in the vicinity of the dipole resonance in the invariant plane $y = 0$ for a spherical particle with $q = 0.3$. The non-dissipative limit $\mathrm{Im}\,\varepsilon'' = 0$. The wave vector of the incident plane linearly polarized wave is parallel to the z axis. Its $\boldsymbol{E}$ vector oscillates along the x axis. Field lines (*white*) are described by equation $dr/d\theta = r\langle S_r\rangle/\langle S_\theta\rangle$. Null isoclines $\langle S_\theta(r,\theta)\rangle$ and $\langle S_r(r,\theta)\rangle$ are shown in *yellow*, and *pink*, respectively. Numerals indicate different singular points. The exact resonance corresponds to $\varepsilon = -2.22$; **a** $\varepsilon = -2.17$; **b** $\varepsilon = -2.20$. Note different scales of panels (**a**) and (**b**)

the characteristic values of the electromagnetic field achieved in the particle and its vicinity at the anomalous scattering.

The discussed 2D picture of the field lines is very informative, but at the same time it may be misleading in somewhat. The point is that looking at it, one may expect that the density of the field lines (the number of lines crossing a straight unite-length segment aligned normal to them, i.e., the 2D flux density) is proportional to the modulus of the Poynting vector $\langle|\boldsymbol{S}(\boldsymbol{r})|\rangle$. Actually, the former has nothing to do with the latter. Due to the Gauss theorem and condition $\mathrm{div}\langle\boldsymbol{S}(\boldsymbol{r})\rangle = 0$ in any non-singular point outside the particle (inside the particle it is true only if $\varepsilon'' = 0$) the density of the field lines is connected with $\langle|\boldsymbol{S}(\boldsymbol{r})|\rangle$ indeed. But it is in the 3D space! In invariant plane $y = 0$ y-component of $\langle\boldsymbol{S}(\boldsymbol{r})\rangle$ vanishes, but this is not the case for $\langle\partial S_y/\partial y\rangle$. Therefore, two-dimensional divergence $\langle\partial S_x/\partial x\rangle + \langle\partial S_z/\partial z\rangle$ in the invariant plane, generally speaking, does not equal to zero, and the 2D flux in the plane is not conserved along "stream tubes" of the Poynting vector.

To understand the full picture of the energy circulation in the near field zone, even in the vicinity of the invariant plane $y = 0$, we have to get out of this plane, considering actual 3D field lines. Two such lines, are shown in Fig. 6.3. Both of them enter the vicinity of focus 6 in Fig. 6.2a. One of the lines approaches the focus from a direction transversal to plane $y = 0$, then sharply transforms into an unwinding spiral, lying almost parallel to this plane, and after a few rotations around the focus goes downstream to $z \to \infty$. The other is deviated by the focus toward the center of the localized plasmon, approaches it, making a lot of rotations as a winding spiral with a very small pitch, then it is ejected from the center, transforming into an unwinding

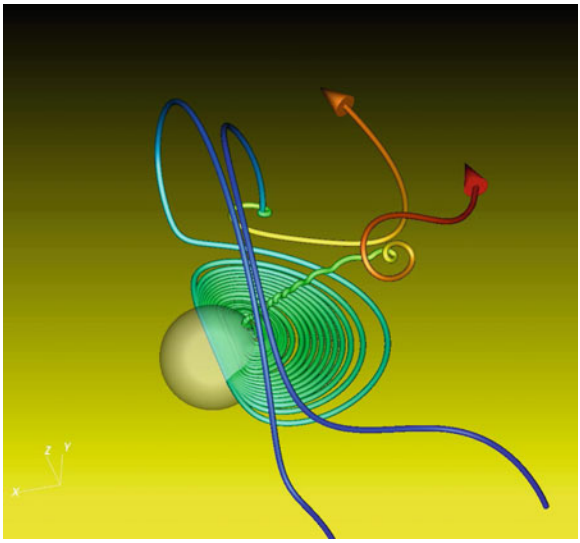

Fig. 6.3 Two 3D field lines lying beyond invariant plane $y = 0$ (*courtesy* of Andrey E. Miroshnichenko). The other details of the problem are identical to those in Fig. 6.2a

spiral with an increasing pitch, and eventually also goes downstream. It means, that the resonant plasmons collect energy not only from the upstream area—a part of it comes from the optical vortexes (points 5 and 6), which lie downstream with respect to the localized plasmons.

Thus, in the vicinity of the resonance the energy circulation corresponds to collection of the energy flux from a large area and delivery of the electromagnetic radiation to the centers of the localized plasmons. The delivery occurs in rather a narrow layer close to invariant plane $y = 0$ and results in huge concentration of the energy in the resonant plasmons. Then, this energy is radiated from the plasmons along directions transversal to the invariant plane, which brings about a powerful emission of electromagnetic field in narrow solid angles, i.e., the plasmons act as very powerful subwavelength floodlights.

All these phenomena take place in the near field zone exclusively and have the characteristic scale of the order of the particle size R. When the distance from the particle increases to the far field zone the scattered field transforms into the conventional field structure typical for the corresponding point dipole. Qualitatively the same picture is valid for other orders of the resonances (quadrupole, octupole, etc.) too.

6.3 Anomalous Absorption

For the time being to inspect the extreme case of the anomalous scattering the main focus of our consideration has been put on the non-dissipative limit. On the other hand, for a number of applications the maximization of the energy release in the particle is important. A naïve answer to the question "How to maximize the absorption cross section of a small particle?" is "To do that maximize the dissipative constant of the particle material, i.e., Im ε." However, the correct answer is just opposite: to achieve the maximal energy release in the particle its dissipative constant should be small. To reveal the physical grounds for that seemingly paradoxical conclusion let us discuss a toy auxiliary problem of the power dissipated at forced oscillations of a pendulum. The equation of motion is as follows:

$$\ddot{x} + 2\nu\dot{x} + \omega_0^2 x = (f/m)\exp(i\omega t),$$

with a steady solution of the form:

$$x = \frac{(f/m)}{\omega_0^2 - \omega^2 + 2i\nu\omega}\exp(i\omega t). \tag{6.16}$$

The mean dissipated power P is the work of the friction force $-2m\nu\dot{x}$ in a unite of time averaged over a period of oscillations. Trivial algebra results in the following expression:

$$P = m\nu\langle\dot{x}\dot{x}^*\rangle = \frac{|f|^2\omega^2\nu}{m[(\omega_0^2 - \omega^2)^2 + 4\nu^2\omega^2]}. \tag{6.17}$$

Suppose that the dissipative constant ν and the driving frequency ω are fixed. Maximization of $P(\omega_0)$ in this case readily yields

$$\max P(\omega_0) = P(\omega) = \frac{|f|^2}{4m\nu} \to \infty \ \text{ at } \ \nu \to 0. \tag{6.18}$$

The reason for the divergence is obvious. While the dissipated power is proportional to the dissipative constant indeed, it is also proportional to square of the amplitude of oscillations, see (6.16), (6.17). At $\omega_0 = \omega$ the latter depends on ν as $1/\nu^2$. Thus, at the point of resonance the product square of the amplitude times the dissipative constant occurs proportional to $1/\nu$ and tends to infinity at $\nu \to 0$.

Precisely the same happens with the dissipated power at the plasmon resonances. The only difference with the discussed toy problem is that the damping rate at the plasmon resonances can never vanish owing to the radiative losses and hence the dissipated power always remains finite. A detailed study of light absorption in this case is presented in [30]. It is shown that the maximal absorption takes place exactly at the frequencies of the plasmon resonances ω_ℓ, corresponding to the roots of equation $G_\ell^{(a)}(\mathrm{Re}\,\varepsilon(\omega)) = 0$. Regarding Im ε, to provide the maximal absorption it should

have such a value that the dissipative damping occurs equal to the radiative one exactly. The corresponding value of Im ε is determined by (6.11), where sign of strong inequality should be replaced by equality.

The physical grounds for this result are very simple. As it has been mentioned, the power dissipated in the particle is proportional to the actual ε'', while the cutoff of a_ℓ at the vicinity of the resonance occurs owing to the effective $\varepsilon''_{\text{eff}}$ which is a sum of the actual ε'' and the non-dissipative term related to the radiative damping, see (6.5). As long as the dissipative losses are smaller than the radiative damping, an increase in the former increases the dissipative constant, but practically does not affect $\varepsilon''_{\text{eff}}$ and hence the amplitude of the resonant field. Then, the overall effect is an increase in the dissipation. In the opposite limit, when the radiative damping is negligible relative to the dissipative losses the case is analogous to the discussed toy model, and an increase in ε'' results in a decrease in the dissipated power, see (6.18). The crossover between the two regimes takes place at the point where the dissipative and radiative dampings are equal each other.

The scattering cross section at this point occurs equal to the absorption one and equal to 1/4 of that given by (6.9). Thus, for the problem in question the quantity

$$\sigma^{(\ell)}_{\text{abs max}} = \frac{\pi}{k^2}\left(\ell + \frac{1}{2}\right) \tag{6.19}$$

corresponds to the absolute theoretical maximum for the partial absorption cross section, which never can be exceeded.[5]

This resonant absorption inherits many features of the anomalous scattering, which allows naming it the *anomalous light absorption*. For example, according to (6.19) $\sigma^{(\ell)}_{\text{abs max}}$ is a certain universal quantity, which does not depend on R and the optical constants of the particle, cf. the corresponding behavior of the extinction cross section at the anomalous scattering, etc.

Estimates show that, as usual, as long as the particle is small ($q \ll 1$) at the ℓth resonance point the contributions of the entire set of the off resonant multipoles is negligible with respect to the resonant partial cross section, and the net resonant absorption cross section is determined by (6.19) with great accuracy.

Thus, in the vicinity of the resonance $\sigma^{(\ell)}_{\text{abs}} = \sigma^{(\ell)}_{\text{abs}}(q, \varepsilon', \varepsilon'')$. However, it is possible to show that introduction of the proper selected dimensionless variables scales out the dependences on ℓ and q, while the dependence on the two remaining variables is reduced to the following simple universal form [30]:

$$\varsigma = \frac{\chi''}{(1+\chi'')^2 + \chi'^2}; \quad \chi'' \geq 0,$$

[5] We stress that (6.9), (6.19) should be regarded as the upper theoretical limit for the corresponding cross sections just for the problem in question (a small spatially uniform non-magnetic particle). In other cases these limits may be exceeded considerably, see, e.g., [34].

where ς, χ' and χ'' stand for the rescaled dimensionless partial absorption cross section, real and imaginary parts of ε, respectively.

6.4 Optimization of Laser Energy Release in Real Plasmonic Nanoparticles

However, application of the results discussed in the previous section to real experiments is not so straightforward. In any real case ε' and ε'' cannot be regarded as two independently varying parameters. The actual tuning parameters are ω and R. To achieve the maximal absorption these parameters must satisfy the set of equations

$$\varepsilon'(\omega, R) = \varepsilon'_\ell(\omega, R), \tag{6.20}$$

$$\varepsilon''(\omega, R) = \varepsilon''_\ell(\omega, R), \tag{6.21}$$

where the left-hand sides follow from the dispersion properties of the particle material[6] while the right-hand sides are given by the conditions for the anomalous absorption: $G_\ell^{(a)}(\varepsilon'(\omega), q) = 0$ and equality of the radiative and dissipative damping, see (6.7), (6.11), respectively. Solutions of (6.20), (6.21) yield a unique set of pairs (ω_ℓ, R_ℓ), where R_ℓ should satisfy the additional constraint following from restriction $q \ll 1$.

It seems that these conditions are very strict, the entire set of them is extremely difficult to fulfill in any real experiment, and hence the limit corresponding to (6.19) is hardly reachable. Fortunately the case is not so dramatic. The point is that usually the functions $\varepsilon'(\omega)$ and $\varepsilon''(\omega)$ are rather smooth, at least as long as metal particles are a concern. On the other hand, while at $q \ll 1$ the dependence $\varepsilon'_\ell(q)$ is weak, see (6.8), the corresponding dependence of the resonant value of ε'' is sharp, see the right-hand-side of (6.11). Then, the following iterative procedure may be built up. First, for a given material we select in its dispersion law $\varepsilon'(\omega)$ the frequencies of the plasmon resonances, which in the zeroth (in q) approximation are determined by the conditions $\varepsilon'(\omega_\ell^{(0)}) = -(\ell+1)/\ell$. Next, we check if among the obtained $\omega_\ell^{(0)}$ there are any, satisfying the condition $\varepsilon''(\omega_\ell^{(0)}) \ll 1$. If this is the case, then, equalizing the left- and right-hand-side parts of (6.11), we find q, corresponding to this value of $\varepsilon'(\omega_\ell^{(0)})$. This q is employed to calculate the corrected solution of equation $G_\ell^{(a)}(\varepsilon'(\omega_\ell), q) = 0$. The obtained corrected $\omega_\ell^{(1)}$ is used to calculate corrected $\varepsilon''(\omega_\ell^{(1)})$, etc. The procedure quickly converges to q_ℓ and ω_ℓ corresponding to the conditions of the anomalous absorption.

If none of $\varepsilon''(\omega_\ell^{(0)})$ is small, the optimization should be performed by a standard numerical method of maximization of a function of several variables. In this case the question "To what extent is the reasoning of the previous section applied to the

[6] R-dependence may appear here owing to γ_{eff}, see (6.12).

results obtained during the maximizarion?" arises. Naturally, the described iterative procedure has just a methodological meaning. In practical calculations it is convenient to apply a single method of maximization, regardless the values of $\varepsilon'(\omega_\ell^{(0)})$. It is also desirable to have quantitative parameters allowing to compare the effectiveness of the resonant laser energy release in a small plasmonic particle relative to the one in the same bulk material.

Let us begin with the second point. The volume density of laser energy release $\mathcal{E}$ [J/cm^3] in a bulk material at the normal incidence of the laser beam is given by the expression:

$$\mathcal{E} = A\alpha\Phi, \tag{6.22}$$

where A is the absorptivity, Φ stands for the fluence of the laser beam [J/cm^2] and $\alpha = 2k\mathrm{Im}\sqrt{\varepsilon} = 2k\kappa$ is the volume absorption coefficient.

On the other hand, the volume density of the laser energy released in the particle averaged over particle volume is given by the expression

$$\mathcal{E} = \frac{3}{4}\frac{Q_{\mathrm{abs}}}{R}\Phi = \alpha_{\mathrm{eff}}\Phi, \tag{6.23}$$

where $\alpha_{\mathrm{eff}} = 3Q_{\mathrm{abs}}/(4R)$. Comparing (6.22) and (6.23), we see that quantitative measures of the effectiveness of the resonant energy release in the particle relative to the bulk material may be the following coefficients [35]:

$$\beta = \frac{\alpha_{\mathrm{eff}}}{\alpha}, \quad \beta_{\mathrm{eff}} = \frac{\alpha_{\mathrm{eff}}}{A\alpha}. \tag{6.24}$$

We name them the *net absorption enhancement factors*. Since $0 \le A \le 1$, the quantity β presents the *minimal* value of the absorption enhancement. If condition $\beta_{\mathrm{eff}} \ge \beta \gg 1$ is met, the nanoparticle absorbs light much more efficiently than the corresponding bulk material. To distinguish the role of partial resonances introduction of the partial enhancement factors $\beta_{\mathrm{eff}}^{(\ell)}$ and $\beta^{(\ell)}$ with the replacement in the definition of α_{eff} in (6.23), $Q_{\mathrm{abs}} \to Q_{\mathrm{abs}}^{(\ell)}$ is also meaningful [35].

To understand to what extent the arguments of the previous section may be applied to natural materials we have optimized numerically β_{eff} for six metals: potassium, aluminum, sodium, silver, gold and platinum, whose properties cover the range from weak dissipation at the optical frequencies (potassium) to the strong one (platinum). The model employed in the calculations was identical to the one discussed in the previous section for the aluminum particle, see (6.12). The results of these calculations obtained for each particle in the vicinity of its dipole resonance ($\ell = 1$) are collected in Table 6.1 [35].

These results exhibit good agreement with the preceding theoretical discussion. All the particles do have the optimal wavelength, lying close to the one for the corresponding plasmon resonance, and the optimal size, lying in the several-nanometer-scale. Larger enhancement of the energy release relative to the corresponding bulk

Table 6.1 Values of the parameters maximizing absorption of nanoparticles made of different metals irradiated by a plane linearly polarized electromagnetic wave in a vacuum; λ_0 corresponds to the frequency, satisfying the plasmon resonance condition at $R \to 0: \ \varepsilon'(\omega) = -2$

Metal	λ_0, nm	$\mathrm{Im}\,\varepsilon(\lambda_0)$	v_F, cm/s	Optimal R, nm	Optimal λ, nm	$\alpha_{\mathrm{eff}}^{\max}$, cm^{-1}	α, cm^{-1} (bulk)	β_{eff}
K	542	0.138	0.86×10^8	14.1	548	5.02×10^6	3.29×10^5	242
Na	377	0.178	1.07×10^8	10.3	381	5.75×10^6	4.74×10^5	151
Al	139	0.16	2.02×10^8	4.4	141	1.38×10^7	1.29×10^6	147
Ag	354	0.6	1.39×10^8	12.2	356	2.40×10^6	5.2×10^5	19.2
Au	485	3.97	1.39×10^8	40.8	505	4.22×10^5	4.83×10^5	1.51
Pt	276	5.64	1.45×10^8	17.9	213	6.48×10^5	9.1×10^5	1.24

materials have particles with smaller values of the dissipative constant at the resonance point, cf. β_{eff} for potassium and platinum.

However, if laser heating of particles is concerned, the discussed optimization of the energy release plays the role of an intermediate result. To find the temperature rise of the particle we must consider the heat transfer from the particle to a host environmental medium. This problem is inspected in the next section.

6.5 Laser Heating of Particles in Liquid

In the present section we discuss heating with a single laser pulse with duration t_u of a metal particle embedded in a transparent liquid. The thermometric constants of the liquid are close to those for water. The initial temperature equals the room one. The temperature rise is limited by several tens Kelvin, so that the boiling temperature is not reached. Such a problem formulation is typical for numerous medical and biological applications, see, e.g., [36–40] and references therein.

Owing to the apparent importance of the problem, it has attracted a great deal of attention of numerous researchers, see, e.g., [41–45]. However, in a standard approach to the theoretical description of the heating (see, e.g., [46]) the problem is formulated as study of heat transfer with a source (energy release in the particle) calculated as a solution of the corresponding diffraction problem. Such a heat transfer problem does not have simple exact analytical solutions, and different studies employ either approximate analytical methods (valid for certain cases only) or direct numerical calculations with the specified parameters. On the other hand, for practical applications it is highly desirable to obtain a simple analytical solution describing the temperature rise at the surface of the particle T_s in a broad domain of variations of the problem parameters, and for the particle sizes ranging from nanometers to millimeters. In the present section we discuss an approximate solution of such a kind presented in recent publication [47].

We suppose that heat diffusion is the only process responsible for energy exchange between the particle and the liquid. Convection processes do not play any role in the problem owing to a large characteristic time required for the convection to arise. We also suppose that the electron and phonon subsystems in the metal particle are in local equilibrium and may be described by single joint temperature. It imposes the restriction on the laser pulse duration $t_u \gg 1/\gamma$ for particles whose size is larger than the electron free path length, where γ stands for electron-phonon collision frequency. For smaller particles relaxation of the electron subsystem occurs because of collisions of the free electrons with the particle's surface. It results in the condition $t_u \gg R/v_F$. Joining of the conditions yields $t_u \gg \min(1/\gamma,\ R/v_F)$. For typical values of the constants $v_F \sim 10^8$ cm/s and $\gamma \sim 10^{13}$ s^{-1} (room temperature) a crossover from condition $t_u \gg 1/\gamma$ to $t_u \gg R/v_F$ occurs at $R \sim 10^{-5}$ cm.

For the sake of simplicity, we restrict our consideration by the Rayleigh scattering, excluding the anomalous absorption as rather an "exotic" effect. It may be readily incorporated into the discussed approach, if required.

Next, we neglect the angular dependence of the heat sources, supposing that the volume density of the sources inside the particle depends just on radial variable r. It allows to replace the actual 3D heat transfer problem by its spherically-symmetric version.

The grounds for this neglect are in the following. The actual angular inhomogeneity in the heat sources for small particles is rather weak due to diffractive distortions of the incident light. It results even in weaker temperature inhomogeneities, owing to the high rate of heat transfer in metals. On the other hand, in what follows we are interested in *estimates* of the maximal temperature rise at the particle surface, rather than in its exact calculations. For this reason we employ the spherically-symmetric problem formulation even for large particles, when the illuminated part of the particle obviously has a temperature higher than that in the shadow.

Under the approximation made the problem is characterized by four spatial scales, namely the particle size R, skin layer thickness δ, characteristic length of heat diffusion in the particle $2\sqrt{a_p t_u}$ and the one in the surrounding medium $2\sqrt{a_m t_u}$. Here a_p and a_m are the thermal diffusivity for the particle and medium, respectively. Interplay of these scales determines the entire variety of different heating regimes. Note also that according to the problem formulation (a metal particle in a water-like liquid) $a_m \ll a_p$.

Let us consider, for example, two cases: (i) $\delta \ll R \ll \sqrt{a_m t_u} \ll \sqrt{a_p t_u}$ and (ii) $\delta \ll \sqrt{a_m t_u} \ll R \ll \sqrt{a_p t_u}$. Condition $\delta \ll R$ means that absorption of light occurs in a narrow surface layer of the particle. In this case the absorption cross section should be proportional to the surface area, i.e., in equality $\sigma_{\text{abs}} = \pi R^2 Q_{\text{abs}}$ quantity Q_{abs} is practically R-independent.

Regarding condition $R \ll \sqrt{a_p t_u}$, it means that the temperature field inside the particle is quasi-steady and should satisfy the Laplace equation. In spherical coordinates the only non-singular solution of this equation is a constant profile, so that $T(r, t)$ at $r < R$ is reduced to $T(t)$, where time t should be regarded as a parameter.

As for the field outside the particle, it is essentially different in cases (i) and (ii). In case (i) it is also quasi-steady and satisfies the Laplace equation. The corresponding solution is $T = T_s(t)R/r$. Equalizing the dissipated power of the laser beam $q_{\text{laser}} = q_0\sigma_{\text{abs}}$ to the one transferring to the liquid $q_{\text{transf}} = -4\pi R^2 k_m(\partial T/\partial r)_R$, where q_0 stands for the laser beam intensity [W/cm^2] and k_m is the liquid thermal conductivity, we easily find

$$T_s = \frac{\sigma_{\text{abs}} q_0(t)}{4\pi R k_m} \equiv \frac{Q_{\text{abs}} R q_0(t)}{4k_m}. \tag{6.25}$$

In case (ii) the temperature field in the liquid is t- and r-dependent. To determine T_s we may employ the energy conservation law. For simplicity, we consider a rectangular laser pulse. To a certain moment of time $t \le t_u$ the energy W absorbed by the particle is $\sigma_{\text{abs}} q_0 t$.

The absorbed energy is consumed to heat the particle (temperature rise T_s) and to heat an adjacent layer of the fluid. The former requires the energy $(4/3)\pi R^3 C_p \rho_p T_s$, the latter $4\pi R^2 2\sqrt{a_m t} C_m \rho_m T_s/2$, (to enhance the accuracy of the estimate we replace the profile of the temperature in the heated layer by its mean value $T_s/2$). Here C_p and C_m are the corresponding specific heats.

Equalizing W to the consumed energy and considering the equality as an equation for unknown T_s, one easily derives

$$T_s(t) = \frac{\sigma_{\text{abs}} q_0 t}{\frac{4}{3}\pi R^3 C_p \rho_p + 4\pi R^2 C_m \rho_m \sqrt{a_m t}} \equiv \frac{Q_{\text{abs}} q_0 t}{\frac{4}{3} R C_p \rho_p + 4\, C_m \rho_m \sqrt{a_m t}}. \tag{6.26}$$

The obtained $T_s(t)$ is a monotonic function of t, so the maximal temperature rise is achieved in the end of the laser pulse. Replacement $t \to t_u$ brings about the corresponding expression for the maximal temperature rise $\max\limits_{0<t<t_u} T_s$ during the entire laser pulse.

Note, that while in case (i) T_s increases with an increase in R, in case (ii) an increase in R results in a decrease in T_s. It means that T_s reaches a maximum at $R \approx 2\sqrt{a_m t_u}$. This is the case indeed, see Fig. 6.4a.

The other cases are treated analogously. As a result simple analytical expressions for every possible heating regime are obtained [47]. A summary of these expressions is presented in Table 6.2.

To understand Table 6.2 we should clarify that, if a parameter is not explicitly specified in a cell of the table, its value may be any permitted for a given column. For example, condition $R \ll \sqrt{a_m t_u}$ in column *Small particles*, $R \ll \delta$ means any of the following three cases: $R \ll \delta \ll \sqrt{a_m t_u}$, $R \ll \sqrt{a_m t_u} \ll \delta \ll \sqrt{a_p t_u}$ and $R \ll \sqrt{a_m t_u} \ll \sqrt{a_p t_u} \ll \delta$. Other cells should be treated in a similar manner.

Surprisingly, these simple expressions provide quite a reasonable accuracy, see Fig. 6.4a, or [47] for more detailed comparison of the analytical and numerical results. Note also that existence of a maximum of T_s at any fixed value of t_u and a certain finite value of R is quite a common feature of the problem, see Fig. 6.4b.

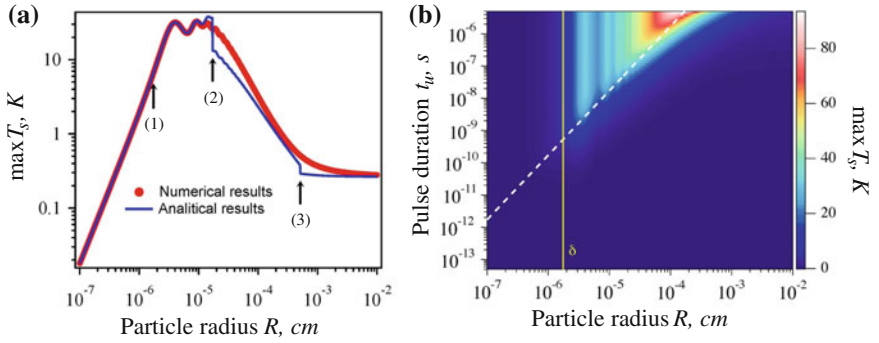

Fig. 6.4 The maximal temperature rise $\max\limits_{0<t<t_u} T_s$ at the surface of a spherical gold particle in water heated by a rectangular laser pulse with wavelength (in vacuum) 532 nm and intensity $q_0 = 5 \times 10^4\,\mathrm{W/cm^2}$. **a** Comparison of the analytical and numerical results $t_u = 50\,\mathrm{ns}$ ($\delta \ll \sqrt{a_m t_u}$). The points of transitions from one heating regime to another are indicated by *black arrows*: (1) $R = \delta$, (2) $R = 2\sqrt{a_m t_u}$, (3) $R = 2\sqrt{a_p t_u}$; **b** The same quantity as a function of the duration of the pulse t_u and the particle radius R. The *dashed line* corresponds to $R = 2\sqrt{a_m t_u}$. Above this line the temperature rise becomes t_u-independent [47]

Table 6.2 Summary of qualitatively different regimes of the laser heating, for small and large metal particles in liquids [47]

Small particles, $R \ll \delta$		**Large particles**, $R \gg \delta$	
Condition	Maximal surface temperature rise	Condition	Maximal surface temperature rise
		Long pulses	
		$R \ll \sqrt{a_m t_u} \ll \sqrt{a_p t_u}$	$\dfrac{Q_{\mathrm{abs}} R q_0}{4k_m}$
$R \ll \sqrt{a_m t_u}$	$\dfrac{Q_{\mathrm{abs}} R q_0}{4k_m}$	$\sqrt{a_m t_u} \ll R \ll \sqrt{a_p t_u}$	$\dfrac{Q_{\mathrm{abs}} q_0 t_u}{\frac{4}{3} R C_p \rho_p + 4\, C_m \rho_m \sqrt{a_m t_u}}$
		$\delta \ll \sqrt{a_p t_u} \ll R$	$\dfrac{Q_{\mathrm{abs}} q_0}{2\sqrt{\pi}} \dfrac{\sqrt{a_p a_m t_u}}{k_p \sqrt{a_m} + k_m \sqrt{a_p}}$
		Short pulses	
$\sqrt{a_m t_u} \ll R$	$\dfrac{Q_{\mathrm{abs}} q_0 t_u}{\frac{4}{3} R C_p \rho_p + 4 C_m \rho_m \sqrt{a_m t_u}}$	$\sqrt{a_p t_u} \ll \delta \ll R$	$\dfrac{Q_{\mathrm{abs}} q_0 t_u}{4(C_p \rho_p \delta + C_m \rho_m \sqrt{a_m t_u})}$

6.6 Conclusion

To summarize the results discussed in the present chapter we may say that recent studies of the old problems of light scattering by small particles and their light heating have revealed many new and sometimes unusual aspects of these problems. Specifically, light scattering by particles with small values of imaginary part of permittivity exhibits in the vicinity of the plasmon resonances the resonant anomalous scattering. Such a scattering is characterized by a giant concentration of the incident light in the particle and its near field zone, so that the characteristic values of the

electric and magnetic fields as well as the one of the Poynting vector occur singular in the particle size.

The extinction cross section at the anomalous scattering achieves the maximal possible for this quantity value. It depends just on the frequency of the incident light, the order of the resonance (dipole, quadrupole, octupole, etc.) and does not depend on the particle size and its optical properties.

At the anomalous scattering the energy circulation in the near field zone corresponds to its delivery to the centers of the localized plasmons with further re-emission of the delivered energy to "infinity". However, this general scenario may be realized in a very complicated manner, when the vector Poynting field has a very unusual structure with a number of singular points. Details of this structure are very sensitive to the detuning of the incident light frequency from the exact plasmon resonant value. It provides a unique opportunity of controlled variations of electromagnetic field on a subwavelength scale.

The anomalous scattering exhibits the inverted hierarchy of resonances, when the resonant cross section and the range of complexity of the vector Poynting field in the near field zone increases with an increase in the order of the resonance.

The anomalous scattering may be accompanied by the resonant anomalous absorption. The anomalous absorption is realized at the plasmon resonance frequencies, when imaginary part of the particle permittivity is a small quantity, satisfying a certain resonant condition. The absorption cross section at the anomalous absorption has the maximal value which cannot be exceeded. At the very point of the anomalous absorption the scattering and absorption cross sections equal each other, while the extinction cross section equals half of the maximal extinction cross section at the anomalous scattering. After the proper scale transformation dependence $\sigma_{\mathrm{abs}}(\varepsilon', \varepsilon'')$ for the anomalous absorption may be reduced to a certain universal form, which does not depend on the particle size and the order of the resonance.

The optimization of the energy release in particles made from various metals shows that for any of them there is a certain pair of the optimal particle size and wavelength of the incident light, maximizing the energy release, where the optimal size is about 10 nm and the corresponding optimal wavelength for different metals in a vacuum varies from green (potassium) to UV (aluminum, platinum) ranges of the spectrum.

The effectiveness of the energy release in the particles with respect to the one in the same bulk material increases with a decrease in imaginary part of the particle permittivity at the optimal wavelength. Thus, the most effective are the particles made from weakly dissipating metals.

The effect of the optimal size takes place at laser heating of a particle embedded in a transparent liquid too. However, in this case it is related to changes of the heating regimes with an increase in the particle size at a fixed value of the laser pulse duration, depends on the latter, optical and thermometric constants of the problem and may vary in broad limits.

We hope the results discussed in the present chapter will help numerous researchers to select the best for given applications particles and irradiation regimes and stimulate further study of this important and fascinating subject.

Acknowledgments This study was partially supported by RFBR, research project No 12-02-00391_a.

References

1. L. Rayleigh, Phil. Mag. **41**, 107, 274, 447 (1871)
2. C.F. Bohren, D.R. Huffman, *Absorption and Scattering of Light by Small Particles* (Willey, New York, 1998)
3. H.C. van de Hulst, *Light Scattering by Small Particles* (Dover, New York, 2000)
4. M.I. Mishchenko, J.W. Hovenier, L.D. Travis (eds.), *Light Scattering by Nonspherical Particles: Theory, Measurements, and Applications* (Academic Press, San Diego, 2000)
5. M.I. Mischenko, L.D. Travis, A.A. Lacis, *Scattering, Absorption, and Emission of Light by Small Particles* (Cambridge University Press, Cambridge, 2002)
6. R. Fuchs, K.L. Kliewer, J. Opt. Soc. Am. **58**, 319 (1968)
7. J.A. Fan et al., Science **328**, 1135 (2010)
8. J.B. Lassiter et al., Nano Lett. **10**, 3184 (2010)
9. F. Hao et al., Nano Lett. **8**, 3983 (2008)
10. J. Zhu et al., Nano Lett. **9**, 279 (2009)
11. S. Tretyakov, *Analytical Modeling in Applied Electromagnetics* (Norwood, MA, Artech House, 2003)
12. A.O. Govorov, W. Zhang, T. Skeini, H. Richardson, J. Lee, N.A. Kotov, Nanoscale Res. Lett. **1**, 84 (2006)
13. A.O. Govorov, H.H. Richardson, Nano Today **2**, 30 (2007)
14. G. Baffou, R. Quidant, C. Girard, Appl. Phys. Lett. **94**, 153109 (2009)
15. J.B. Khurgin, G. Sun, J. Opt. Soc. Am. B **26**, 83 (2009)
16. H.A. Atwater, A. Polman, Nat. Mater. **9**, 205 (2010)
17. G. Baffou, R. Quidant, F.J. Garcia de Abajo, ACS Nano **4**, 709 (2010)
18. V. Giannini, A.I. Fernandez-Domnguez, S.C. Heck, S.A. Maier, Chem. Rev. **111**, 3888 (2011)
19. G. Baffou, H. Rigneault, Phys. Rev. B **84**, 035415 (2011)
20. X. Li, N.P. Hylton, V. Giannini, K.-H. Lee, N.J. Ekins-Daukes, S.A. Maier, Opt. Express **19**, A888 (2011)
21. S. Barlett, W.W. Duley, Astrophys. J. **464**, 805 (1996)
22. L.D. Landau, E.M. Lifshitz, *Electrodynamics of Contineous Media* (Pergamon Press, Oxford, 1989) §8
23. N. Herlofson, Arkiv foer Fysik **3**, 257 (1951)
24. M.I. Tribelsky, A.E. Miroshnichenko, Y.S. Kivshar, Europhys. Lett. **97**, 44005 (2012)
25. B.S. Luk'yanchuk, M.I. Tribelsky,2 *Anomalous Light Scattering by Small Particles and Inverted Hierarchy of Optical Resonances* in Collection of papers dedicated to memory of Prof. M. N. Libenson (The St.-Petersburg Union of Scientists, Russia, 2005) pp. 101–117 (in Russian)
26. M.I. Tribelsky, B.S. Luk'yanchuk, Phys. Rev. Lett. **97**, 263902 (2006)
27. M.I. Tribel'skiĭ, JETP **59**, 534 (1984)
28. Z.B. Wang et al., Phys. Rev. B. **70**, 035418 (2004)
29. E.D. Palik, *Handbook of Optical Constants of Solids* (AP, New York, 1985–1998)
30. M.I. Tribelsky, Europhys. Lett. **94**, 14004 (2011)
31. M.V. Bashevoy, V.A. Fedotov, N.I. Zheludev, Opt. Express **13**, 8372 (2005)
32. B.S. Luk'yanchuk, M.I. Tribel'skiĭ, V. Ternovskiĭ, J. Opt. Technol. **73**, 7 (2006)
33. B.S. Luk'yanchuk, et al., EEE Photonics Global@Singapore (IPGS), vols. 1&2, pp. 187–190 (2008)
34. Z. Ruan, S. Fan, Phys. Rev. Lett. **105**, 013901 (2010)
35. B.S. Luk'yanchuk et al., New J. Phys. **14**, 093022 (2012)
36. X. Huang, P.K. Jain, I.H. El-Sayed, M.A. El-Sayed, Lasers Med. Sci. **23**, 217228 (2008)

37. I. Brigger, C. Dubernet, P. Couvreur, Adv. Drug Deliv. Rev. **54**, 631651 (2002)
38. R.R. Anderson, J.A. Parrish, Science **220**, 524–527 (1983)
39. G. Han, P. Ghosh, M. De, V.M. Rotello, NanoBioTechnology **3**, 40–45 (2007)
40. A.G. Skirtach, C. Dejugnat, D. Braun, A.S. Susha, A.L. Rogach, W.J. Parak, H. Möhwald, G.B. Sukhorukov, Nano Lett. **5**, 13711377 (2005)
41. A.N. Volkov, C. Sevilla, L.V. Zhigilei, Appl. Surf. Sci. **253**, 6394–6399 (2007)
42. H.H. Richardson, M.T. Carlson, P.J. Tandler, P. Hernandez, A.O. Govorov, Nano Lett. **9**, 1139–1146 (2009)
43. G.W. Hanson, S.K. Patch, J. Appl. Phys. **106**, 054309 (2009)
44. E. Sassaroni, K.C.P. Li, B.E. O'Neill, Phys. Med. Biol. **54**, 5541 (2009)
45. S. Bruzzone, M. Malvaldi, J. Phys. Chem. **113**, 15805 (2009)
46. G. Baffou, H. Rigneault, Phys. Rev. B **84**, 035415-1-13 (2011)
47. M.I. Tribelsky et al., Phys. Rev. X. **1**, 021024 (2011)